

# HOW RESIDUAL STRESSES AFFECT PREDICTION OF BRITTLE FRACTURE

**Michael R. Hill**

Mechanical and Aeronautical Engineering Department  
University of California, Davis  
mrhill@ucdavis.edu

**Tina L. Panontin**

Systems Engineering Division  
NASA Ames Research Center  
tpanontin@mail.arc.nasa.gov

## ABSTRACT

It is generally accepted that residual stresses present in welded joints alter the conditions for fracture initiation by contributing to the crack-driving force. In this study, it is shown that weld residual stresses also alter crack-tip constraint, affecting fracture in an additional way. The fracture behavior of two crack geometries, a large pressure shell and a small fracture specimen, both containing an idealized welding residual stress state, is examined computationally. Results are discussed in terms of the effect of the residual stresses on fracture prediction.

## NOMENCLATURE

$J$	$J$ -integral
$K_I$	Mode-I stress intensity factor
$Q$	Constraint parameter
$\sigma_o$	Uniaxial yield strength
$t$	Pipe wall thickness
$a$	Defect size
$b$	Ligament size ( $b = t - a$ )
$R$	Pipe radial distance
$K^{Total}$	Stress intensity factor including residual stress
$K^{Appl}$	Stress intensity factor due to applied load
$K^{RS}$	Stress intensity factor due to residual stress
$J^{Total}$	$J$ -integral due to applied load and residual stress
$J_{el}^{Appl}$	Elastic part of the $J$ -integral due to applied load
$J_{pl}^{Appl}$	Plastic part of the $J$ -integral due to applied load
$J^{RS}$	$J$ -integral due to residual stress
$J_c$	$J$ -integral at fracture initiation
$r, \theta$	Polar coordinates with origin at the crack-tip
$\sigma_{yy}$	Crack opening stress
$l^*$	Characteristic length scale in the RKR failure model

$\sigma_f^*$	Critical stress in the RKR failure model
$P_c$	Applied load that causes $J = J_c$

## INTRODUCTION

Prediction of brittle fracture is often performed by assuming that global fracture parameters such as the  $J$ -integral,  $J$ , or the Mode-I stress intensity factor,  $K_I$ , control the fracture event. The usual method in the presence of a known residual stress field is to use superposition. However, this approach assumes  $J$  or  $K_I$  controlled fracture and therefore ignores the influence of *constraint* which affects the magnitude of the crack-tip stress fields. Two bodies loaded to the same value of the global fracture parameter, but under differing levels of constraint, will contain different crack-tip stresses. Because crack-tip stresses are altered, constraint effects have been shown to cause large changes in brittle fracture toughness.

It is well known that different levels of constraint can exist in structures due to differences in geometry (e.g., thick versus thin) or applied loading (e.g, tension versus bending). Less understood is that constraint changes can also occur due to the presence of residual stress. Previous computational studies by the authors (Panontin and Hill, 1996) (Hill and Panontin, 1997) have demonstrated through the use of  $J$ - $Q$  analysis that triaxial residual stresses typical of welding not only affect the crack driving force at a given load but also induce toughness changes at brittle fracture loads by directly altering constraint.

The focus of this paper is to use the authors' previously reported results to demonstrate how superposition can lead to erroneous fracture prediction in residual stress bearing mild steel. The approach pursued uses the finite element method (FEM) to provide the elastic-plastic crack-tip stress state as a function of increasing applied load and  $J$ -integral in two crack geometries. These data are used within a micromechanical model to predict when the conditions for brittle fracture are satisfied. The global ( $J$ -integral) and local

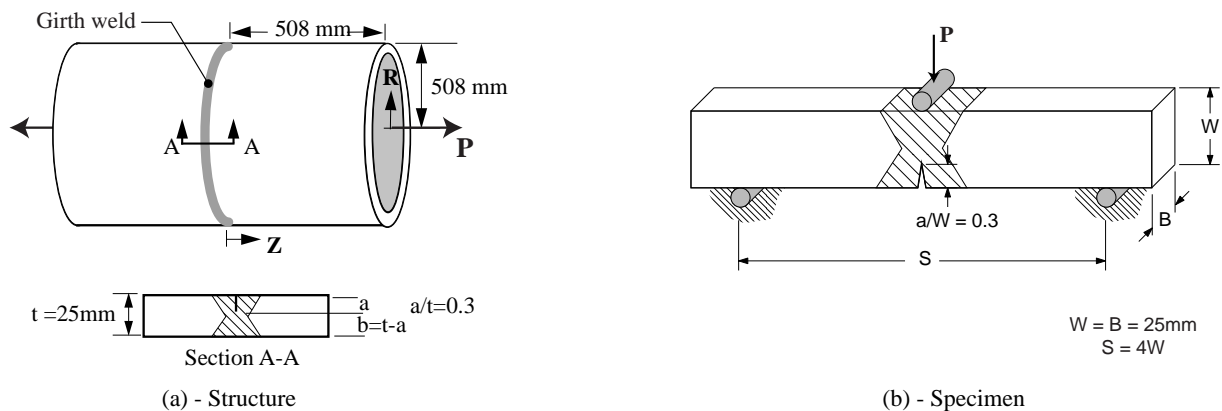


Figure 1 – (a) Axially-loaded externally-cracked pipe and (b) SE(B) specimen.

(micromechanics) predictions of fracture are then compared in terms of the applied load required to initiate fracture.

## CRACK GEOMETRIES

The two crack geometries investigated are shown in Figure 1. Homogeneous material properties are assumed, so that the influence of residual stress on fracture can be isolated. Material response is assumed to be elastic-plastic and to correspond with the behavior of normalized A516-70. This material is a high hardening, ferritic, pressure vessel steel with a uniaxial yield strength,  $\sigma_o$ , of 303 MPa.

In the current context, the girth-welded pipe represents a “structure”, while the SE(B) geometry represents a “specimen”. We assume that the specimen is removed from the structure and fabricated such that the flaw is situated relative to the weld bead in the same way as it lies in the structure (i.e., crack-opening transverse to the weld and propagation in the weld thickness direction). Although residual stress is caused by the same source (welding) in each body, residual stress will be different because stresses are released when a specimen is removed from a structure. In each geometry, then, residual stresses will affect driving force and constraint differently. Accordingly, changes in fracture behavior from specimen to structure will arise due to geometry and loading differences as well as differences in residual stresses.

## RESIDUAL STRESS DISTRIBUTION

Residual stresses arise from most mechanical or thermal operations performed in processing engineering materials. For welding, residual stresses are caused by the thermal cycle that occurs when hot weld metal is laid on much cooler base metal or previous weld passes. Subsequent cooling causes thermal, plastic, and transformation strains to set up in the material, and these strains give rise to residual stress. Residual stress is in fact entirely determined by the geometry of the structure and the distribution of *eigenstrain*, a combination of all the non-elastic, incompatible strains set up during the welding cycle (Mura, 1987). The eigenstrain field (a tensor with spatial dependence) induced by a particular welding process must be found either experimentally (Hill, 1996) or using modeling. However,

once the eigenstrain field is known, residual stress at every point within a welded structure can be found from a *linear elastic* analysis using the theory of elasticity or an approximation such as the finite element method (Hill, 1996).

The use of an eigenstrain distribution offers several advantages for further analysis. First, the residual stress present in a welded structure can be determined by imposing the eigenstrain distribution in a linear elastic finite element model of the geometry. Although that analysis is complicated by the spatial variation of each component of the eigenstrain tensor, a general-purpose finite element program can be used to produce the residual stress estimates. Secondly, the removal of a sample (e.g., the SE(B)) from the larger structure can be simulated by simply imposing the eigenstrain distribution in the removed sample geometry (i.e., the cutting process is assumed to produce only *elastic* deformations). Using this approach, the elastic release of stress which accompanies sample removal from the larger structure is accounted for. Therefore, making use of a known eigenstrain distribution allows the residual stresses to be easily determined in both the welded structure and the fracture specimen removed from that structure. Further, when the eigenstrain field is known the entire, full-field, triaxial residual stress state is known at every point within both the original structure and any removed specimen.

Here we make use of an assumed eigenstrain distribution. This distribution gives rise to residual stresses that are typical of a continuously welded, *double-sided* joint in mild steel plate (Gunnert, 1961). The nature of continuous welding allows the assumption of an eigenstrain field that depends on the transverse and perpendicular welding directions but is independent of position along the welding direction.

The residual stress field computed when the assumed eigenstrain field is imposed in an *un-flawed* pipe geometry is shown in Figure 2, on the plane where the crack will be introduced. For the flaw shown in Figure 1(a), axial stresses tend to open the crack and over the length of defect considered (from 0 to 0.3 in Figure 2), the axial residual stress is tensile. Accordingly, residual stresses will tend to increase the crack-driving force and therefore decrease the fracture load for the pipe.

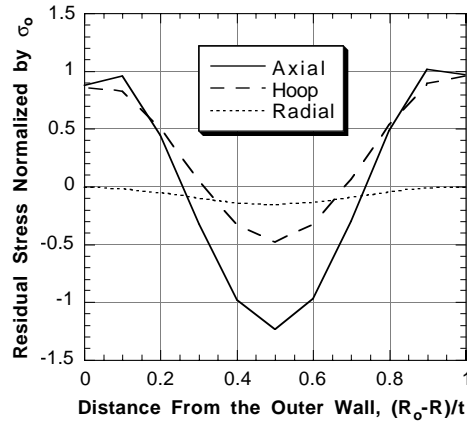


Figure 2 – Residual stress in the pipe on the crack plane.

As shown, axial and hoop residual stresses are tensile on the inner and outer surfaces of the pipe, and compressive at the mid-wall. Both reach a maximum level of the yield strength of the plate; the axial stresses also reach yield strength level in compression. Radial stresses are small. Although not shown in Figure 2, the surface residual stress state gradually decays to zero over a distance from the crack plane approximately equal to the wall-thickness. These characteristics of thick, as-welded, multi-pass, double-sided welds have been well documented (Gunnert, 1961). Here, the eigenstrain field is idealized in the sense that it is symmetric about both the centerline of the weld and the mid-wall. Because welding is generally performed from one side in piping systems, this field is not typical of welded pipe. However, in large pressure shells (e.g. wind tunnels), larger diameter sizes allow the type of two-sided welding that generates the residual stress field examined. This is a major source of the difference between the residual stress field shown in Figure 2 and that expected in girth welded pipes (e.g., see Rybicki (1986)).

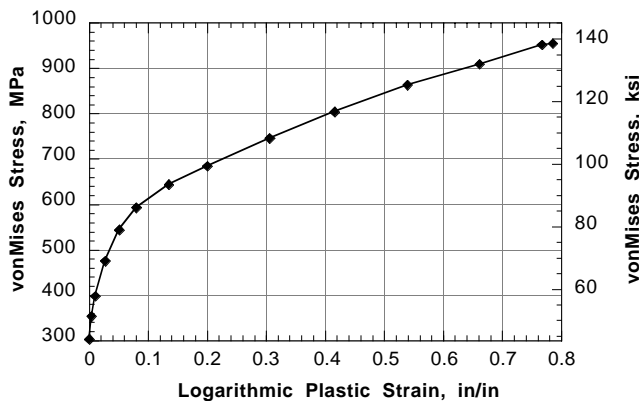


Figure 3 – Flow properties for normalized A516-70

## ANALYSIS TECHNIQUE

Elastic-plastic finite element computation is used to simulate the response of the bodies shown in Figure 1 to both applied and residual stresses. The finite element solutions employ a non-linear, finite strain formulation. For simulations in the presence of residual stresses, the eigenstrain distribution is first imposed in each body with crack-face nodes restrained. Once equilibrium of the residual stress state is found, these tractions are released, allowing the crack to open and simulating the effect of fatigue pre-cracking. The final step is to impose the applied loading. Plasticity is assumed to follow isotropic, incremental  $J_2$  flow theory with a piece-wise linear Cauchy-stress logarithmic-strain curve obtained from tensile testing and shown in Figure 3. As mentioned above, each body is assumed to be homogeneous so that differences between weld and plate material are not modeled. The  $J$ -integral is estimated at each increment of applied loading using the domain-integral technique. As such, the computed  $J$ -values include the contribution of residual stress. Further details on the finite element meshes employed, material properties assumed and residual stress distributions imposed in each geometry can be found in the authors' previous studies (Hill and Panontin, 1997) (Panontin and Hill, 1996).

## FRACTURE PREDICTION USING SUPERPOSITION

To account for the influence of a known residual stress state on fracture in an elastic body using superposition analysis, the total stress intensity factor (SIF) due to a combination of applied load and residual stress is found by

$$K^{Total} = K^{Appl} + K^{RS} \quad [1]$$

$K^{RS}$  for a known residual stress field can be found for an elastic body by employing Bueckner's weight function (Bueckner, 1958). For an elastic-plastic body, the situation is more difficult and several approaches have been suggested in the literature. EPRI recommends an expression similar to Equation [1] (Kumar, et al, 1981) but involving  $J$

$$J^{Total} \approx \{ \sqrt{J_{eI}^{Appl}} + \sqrt{J_{eI}^{RS}} \}^2 + J_{pl}^{Appl} \quad [2]$$

Equation [2] provides a reasonable estimate of  $J^{Total}$  only in small-scale yielding because the crack-driving force due to residual stress,  $J_{RS}$ , is assumed only to contribute to the elastic part of the  $J$ -integral and not to change with increasing load. Other, more involved approaches to failure assessment account for residual stresses in similar ways. Milne, et al (1988) call for inclusion of a "load interaction factor" (also called the "rho-factor") to correct for the influence of plasticity. The present study paper does not consider a load interaction factor.

To employ superposition, the initiation of cleavage fracture is predicted to occur when

$$J^{Total} \geq J_c \quad [3]$$

where  $J_c$  is the material toughness obtained from testing. Equation [3] does not explicitly account for the influence of constraint and its use may lead to inaccurate fracture prediction. It may be possible to improve Equation [3] by adjusting  $J_c$  to include constraint effects. The efficacy of this approach in the presence of residual stresses will be discussed below.

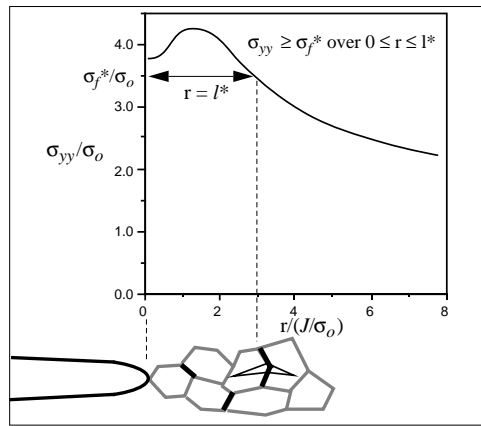


**Figure 4** – Schematic representation of the RKR micromechanical fracture model.

### FRACTURE PREDICTION USING MICROMECHANICS

Cleavage fracture in mild steels can also be predicted using a micromechanical model. The RKR model (Ritchie, et al, 1979), illustrated in Figure 4, predicts fracture when the opening stress,  $\sigma_{yy}$ , ahead of the crack-tip exceeds a fracture stress,  $\sigma_f^*$ , over a critical distance,  $l^*$ . This model employs FEM to predict crack-tip stresses and is implemented here by examining the FEM-predicted evolution of opening stress ahead of the crack-tip, whether due to applied loading alone or in combination with residual stress. When the micromechanics condition for fracture initiation is satisfied, the associated applied load and global fracture parameters (e.g.,  $J$ -integral) are found from the FEM results. In the current study, the RKR parameters are assumed to be  $\sigma_f^* = 3.5\sigma_o$  and  $l^* = 0.15$  mm, about 3 ferritic grain diameters in A516-70 (Panontin and Hill (1996)).

### CONSTRAINT ANALYSIS

The change in constraint conditions due to geometry and the influence of the residual stress field can be quantified using  $J$ - $Q$  theory. The theory uses an approximate two-parameter description of the crack-tip stress-strain fields developed from asymptotic analyses and finite element simulations performed by O’Dowd and Shih (1991 and 1992). These stress fields are applicable to small and large scale yielding conditions and can be written as

$$\sigma_{ij} = \sigma_o f_{ij}(r/(J/\sigma_o), \theta, Q) \quad [4]$$

where  $r$  and  $\theta$  are polar coordinates centered at the crack-tip and the parameter  $Q$  is dimensionless. As a measure of how much  $\sigma_{ij}$  differs from the adopted small scale yielding (SSY) reference solution at the same applied  $J$ , the parameter  $Q$  has been shown to characterize the magnitude of the hydrostatic stress over the forward sector ahead of the crack-tip (i.e.,  $\theta < \pi/2$  and  $1 < r/(J/\sigma_o) < 5$  to a good approximation.  $Q$  is formally defined as

$$Q = [\sigma_{\theta\theta} - \sigma_{\theta\theta}|_{SSY}] / \sigma_o \text{ at } \theta = 0, r/(J/\sigma_o) = 2 \quad [5]$$

and is obtained from stresses predicted straight ahead of the crack-tip by finite element analyses of both finite and infinite size (SSY) crack geometries. For bodies loaded purely in Mode I,  $Q = 0$  in all crack geometries under small scale yielding conditions. However, as deformation levels increase in finite size specimens, the hydrostatic stresses at the crack-tip are relieved and fall below those that exist in an infinite cracked body at the same  $J$ -value. This produces a negative  $Q$ -value, which denotes a loss in constraint. A positive  $Q$ -value indicates that high constraint exists for a particular geometry and loading condition.

In this study, we choose to compute  $Q$  further away from the crack-tip than the standard distance of  $r/(J/\sigma_o) = 2$  because, in the analysis of brittle fracture, the stress state at small values of  $J$  is required, calling for stress estimates at extremely small distances ahead of the crack-tip,  $r$ . Even with the crack-tip element size of 0.0076 mm (0.0003 inch) used in this study, use of  $r/(J/\sigma_o) = 4$  is required to obtain accurate estimates of  $Q$  early in the loading history.

## RESULTS

### Micromechanical fracture prediction

Fracture predictions using the superposition and RKR methods are reported in Table 1. At the load corresponding to RKR-predicted fracture, crack-tip opening stresses are nearly the same in each different geometry. As can be seen in Column 2 of Table 1, this occurs at markedly different values of  $J$ . For the two non-residual-stress, or “unwelded”, cases there is a large difference in RKR-predicted  $J$  at fracture,  $J_c$ . This demonstrates an anticipated constraint effect since the tension-loaded pipe is significantly less constrained than the SE(B) specimen. Constraint-loss increases crack-tip plasticity, so that additional loading is required to reach a critical crack-tip stress state.

For the “welded” cases, which include residual stress, the RKR model predicts a decrease in  $J_c$  from the unwelded case. The decrease in  $J_c$  is due to residual stresses acting to suppress crack-tip plasticity. Figure 5 shows the equivalent plastic strain distribution with distance straight ahead of the crack-tip for the pipe geometry subject to applied loading alone (Pipe) and to applied loading in combination with residual stress (Welded Pipe), each loaded to the same value of  $J$ . The *constrained* deformation (lower plastic strain) in the welded pipe leads to higher crack-tip opening stresses than exist in the unwelded pipe loaded to the same  $J$ . Since the RKR prediction is based on stress, this explains why the RKR-predicted  $J_c$  is lower for the welded than for the unwelded pipe. The constraint generated by residual stress causes a 63% decrease in toughness for the pipe while for the SE(B) geometry the toughness decrease is 26%. The large difference in residual stress induced toughness change for each geometry is thought to result from the relative absence of longitudinal welding residual stress in the SE(B) specimen, stresses which act in the hoop direction in the pipe and are released when the SE(B) is cut free.

### J-Q analysis

The effect of geometry and residual stress on crack-tip constraint is also reflected in the  $J$ - $Q$  trajectories for each specimen, shown in Figure 6. The final point (largest  $J$ ) on each curve represents the point of RKR predicted fracture initiation. The trend in the final point on

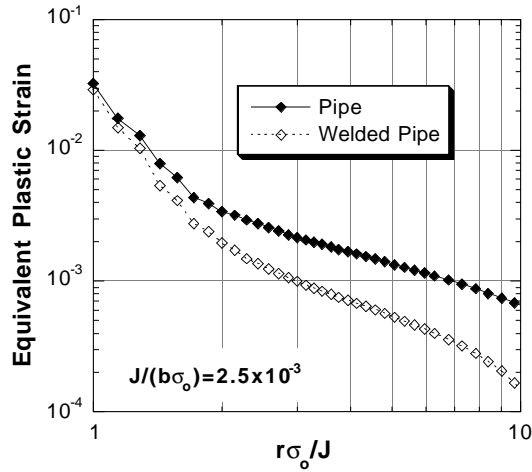


**Figure 5** – Distribution of equivalent plastic strain with distance ahead of the crack-tip. (Pipe, with and without residual stress, both loaded to the same value of  $J$ .)

each  $J$ - $Q$  trajectory (shown hatched) predicts a decrease in  $J_c$  with increasing  $Q$  which is the expected influence of constraint on fracture. However, whether the trend in  $J_c$  shown is representative of the actual fracture behavior of A516-70 is unknown.

In Figure 6, we clearly see that welding residual stress impacts  $Q$ . The unwelded SE(B) specimen starts with  $Q$  near zero and loses constraint slowly (i.e.,  $Q$  decreases) with increasing load due to increasing plasticity. The welded SE(B) starts with a positive value of  $Q$ , and this value decreases more slowly than was the case for the unwelded specimen. This behavior confirms that higher initial constraint ( $Q$ ) present in the welded SE(B) suppresses plastic flow relative to the behavior of the same specimen without RS. We also see clearly in the  $J$ - $Q$  plot how residual stresses directly affect the development of the crack-tip opening stress with increasing load.

The trend in  $J$ - $Q$  space for the structural geometry is different than that of the specimen. The unwelded pipe develops negative  $Q$  even in the early stages of loading, which shows it to be a fairly unconstrained geometry. Because of low initial constraint in the unwelded pipe,  $Q$  continues to decrease with increasing load. The addition of welding residual stress causes a large increase in crack-tip

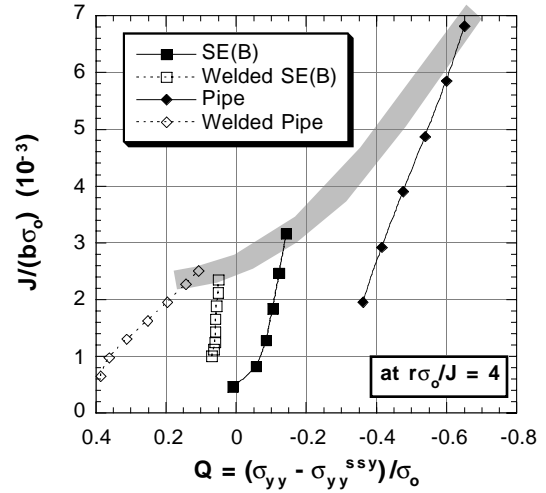


**Figure 6** – Results of  $J$ - $Q$  analysis for the SE(B) specimen and the pipe structure, each with and without residual stresses.

constraint in the pipe, much larger than occurred in the SE(B). Higher constraint in the welded pipe is relieved with increasing  $J$ , at a rate more rapid than for the unwelded pipe. Fracture in the welded pipe occurs at a similar constraint level as for the welded SE(B). This interesting observation is likely serendipitous because the difference in residual-stress-induced constraint is nearly equal and opposite to the difference in geometric constraint between the SE(B) and pipe. Such a coincidence should not be expected in general, and would likely not happen for any other structural geometry.

### Superposition fracture prediction

From the results already presented, it is clear that residual stress impacts fracture in two important ways: by affecting the crack driving force and by altering constraint. Given the different values of RKR-predicted toughness for each case, it should be expected that an approach to fracture prediction that assumes  $J$ -control of crack-tip stresses will be inaccurate. However, it is often thought that a prediction scheme based on  $J$  will at least provide a conservative estimate of the fracture load. In the following discussion, the accuracy of a superposition prediction of fracture is examined, relative to the RKR prediction. Here we assume that the RKR model provides a

Body	$J_c$		Failure Load, $P_c$		
	RKR	RKR	Superposition with RKR $J_c$ from:		
			SE(B)	Pipe	Welded SE(B)
SE(B)	17.0 kN/m	35.0 kN	--	--	--
Welded SE(B)	12.6 kN/m	11.7 kN	--	--	--
Pipe	36.7 kN/m	21.3 MN	17.9 MN	--	--
Welded Pipe	13.5 kN/m	9.83 MN	12.2 MN	19.9 MN	9.11 MN

**Table 1:**  $J$ -integral at fracture (computed using the domain integral) and fracture load predicted using the RKR and superposition models

reliable fracture estimate and compare the RKR and superposition results. This analysis does not use Equation [2] and instead makes use of  $J$ -integral results obtained from the FEM computation. As such, the computation of  $J$  includes the effect of load interaction and the reduction of residual stress with increasing applied load. Errors in the superposition fracture estimates are therefore due only to the assumption of  $J$ -controlled crack-tip stresses.

Using standard procedures,  $J_c$  is typically determined by SE(B) specimen testing. For the unwelded SE(B) specimen in the current study, such a test would yield  $J_c = 17.0$  kN/m (Table 1). For the unwelded pipe, FEM predicts  $J^{Total} = J_c$  (17.0 kN/m) at a load  $P_c = 17.9$  MN. This load estimate is conservative by 16%, relative to the RKR prediction of 21.3 MN. The prediction is in error because it assumes  $J$ -control of crack-tip stresses and ignores constraint-loss in the axially-loaded pipe relative to the SE(B). Again using  $J_c$  obtained from the unwelded SE(B), but now to predict fracture in the welded pipe, we find  $J^{Total} = J_c$  at  $P_c = 12.2$  MN. This load estimate is *non-conservative* by 24%, relative to the RKR prediction of  $P_c = 9.83$  MN. The superposition prediction is in error because it ignores both the constraint-loss due to geometry and constraint generated by residual stress.

It is possible to adjust the superposition predictions by choice of a properly defined  $J_c$ , which is essentially the concept of two-parameter fracture mechanics. For example, if the RKR prediction of fracture in the unwelded pipe is used to account for geometric constraint-loss, we can define  $J_c = 36.7$  kN/m. If we then use superposition to account for residual stresses, we find  $J = J_c$  at  $P_c = 19.9$  MN for the welded pipe. This load is *non-conservative* by 102% because it ignores the constraint generated by residual stress.

Using the RKR  $J_c$  for the welded SE(B) (12.6 kN/m) in a superposition prediction of fracture in the welded pipe provides the best fracture estimate; however, this appears coincidental because it ignores both geometrically induced and residual stress induced constraint changes.

## DISCUSSION

A superposition approach which accounts for both the effect on driving-force and on constraint might be developed. Such an approach would depend on the determination of both  $J_{RS}$  and  $Q_{RS}$  from the residual stress state acting alone.  $Q_{RS}$  might be defined as the difference in  $Q$  between a structure with and without residual stress at some small applied load, similar to the definition of  $J_{RS}$ . However, in the present study the difference in  $Q$  between the unwelded and welded cases changes with  $J$ , even at relatively small levels of  $J$ . Therefore, the value of  $Q_{RS}$  would depend on the load-level used to define it. Accordingly, such an approach may not provide a reliable prediction.

The superposition approach, as currently implemented, can be used to account for the influence of residual stress on driving force. Determining the influence of residual stress on constraint, without the type of non-linear analysis reported on here, requires further investigation. Furthermore, the use of superposition to account for changes in driving force alone can lead to *non-conservative* fracture estimates. It appears that the only accurate way to predict the effect of triaxial residual stress on fracture may be to employ a micromechanical failure methodology, which requires detailed

non-linear analysis to determine the crack-tip stress-strain history with increasing applied load.

In summary, constraint induced by residual stresses can have an important influence on the brittle fracture process. Any fracture prediction scheme based on superposition of crack-driving forces alone does not account for residual stress induced constraint and can therefore produce erroneous results. In ductile fracture, however, this effect has been shown to be much less pronounced (Panontin and Hill, 1996).

## REFERENCES

- Bueckner, H. F. (1958), "The Propagation of Cracks and the Energy of Elastic Deformation," Transactions of the ASME, Series A-D 80, pp. 1225-1230.
- Gunnert, R. (1961), "Residual Stresses," Proceedings of the Special Symposium on the Behavior of Welded Structures, Urbana, IL, University of Illinois Engineering Experiment Station, pp. 164-201.
- Hill, M. R. (1996). Determination of Residual Stress Based on the Estimation of Eigenstrain, Stanford University.
- Hill, M. R. and T. L. Panontin (1997), "Effect of Residual Stress on Brittle Fracture Testing," *Fatigue and Fracture Mechanics: 29th Volume, ASTM STP 1321*, West Conshohocken, PA, ASTM (to appear).
- Kumar, V., M.D. German, and C.F. Shih (1981), An Engineering Approach for Elastic-Plastic Fracture Analysis. EPRI Report NP-1931, Electric Power Research Institute, Palo Alto.
- Milne, I., R. A. Ainsworth, A. R. Dowling, and A. T. Stewart (1986), "Assessment of the integrity of structures containing defects," CEBG Report No. R/H/R6 - Revision 3; Also published in *International Journal of Pressure Vessels and Piping*, 32, pp. 2-104, 1988.
- Mura, T. (1987), *Micromechanics of Defects in Solids*, Dordrecht, Netherlands, M. Nijhoff.
- O'Dowd, N. P., and C. F. Shih (1991), "Family of Crack-Tip Fields Characterized by a Triaxiality Parameter: Part I-Structure of Fields," *Journal of the Mechanics and Physics of Solids* 39 pp. 989-1015.
- O'Dowd, N. P., and C. F. Shih (1992), "Family of Crack-Tip Fields Characterized by a Triaxiality Parameter: Part II-Fracture Applications," *Journal of the Mechanics and Physics of Solids*, 40 pp. 939-963.
- Panontin, T. L. and M. R. Hill (1996), "The effect of residual stresses on brittle and ductile fracture initiation predicted by micromechanical models," *International Journal of Fracture* 82: pp. 317-333.
- Ritchie, R. O., W. L. Server, and R. A. Wullarert (1979), "Critical Fracture Stress and Fracture Strain Models for the Prediction of Lower and Upper Shelf Toughness in Nuclear Pressure Vessel Steels," *Metallurgical Transactions* 10A pp. 1557-1570.
- Rybicki, E. F. and J.R. Shadley (1986), "A Three-dimensional Finite Element Evaluation of a Destructive Experimental Method of Determining Through-thickness Residual Stresses in Girth Welded Pipes," *Journal of Engineering Materials and Technology* 108(2) (1986) pp. 99-106.